NASA TECHNICAL NOTE
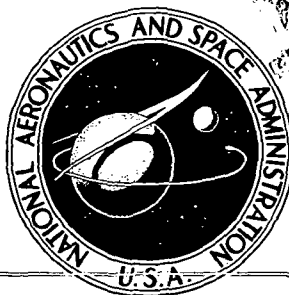
NASA TN D-7253

CASE FILE COPY

ROLE OF PLASTIC DEFORMATION IN WEAR OF COPPER AND COPPER - 10-PERCENT-ALUMINUM ALLOY IN CRYOGENIC FUELS

by Robert C. Bill and Donald W. Wisander

Lewis Research Center
and
U.S. Army Air Mobility R&D Laboratory
Cleveland, Ohio 44135

Page Intentionally Left Blank

1. Report No. NASA TN D-7253	2. Government Accession No.	3. Recipient's Catalog No.
4. Title and Subtitle ROLE OF PLASTIC DEFORMATION IN WEAR OF COPPER AND COPPER - 10-PERCENT-ALUMINUM ALLOY IN CRYOGENIC FUELS		5. Report Date April 1973
		6. Performing Organization Code
7. Author(s) Robert C. Bill and Donald W. Wisander		8. Performing Organization Report No. E-7314
		10. Work Unit No. 501-24
9. Performing Organization Name and Address NASA Lewis Research Center and U.S. Army Air Mobility R&D Laboratory Cleveland, Ohio 44135		11. Contract or Grant No.
		13. Type of Report and Period Covered Technical Note
12. Sponsoring Agency Name and Address National Aeronautics and Space Administration Washington, D.C. 20546		14. Sponsoring Agency Code

15. Supplementary Notes

16. Abstract

High-purity copper specimens and a copper - 10-percent-aluminum alloy specimen were subjected to sliding against 440C in cryogenic fuel environments. It was found that virtually all wear occurred by the plastic deformation of a recrystallized layer extending to about 10 micrometers below the wear scar surface of the copper or copper alloy. The wear debris was in the form of a layered structure adhering to the exit region of the wear scar. Measurements on the high-purity copper specimens indicated that the wear rate was proportional to the applied load and to the sliding velocity squared. A physical model of the wear process is proposed to account for these observations.

17. Key Words (Suggested by Author(s)) Wear Cryogenic fuels Plastic deformation Recrystallization Copper Plane strain		18. Distribution Statement Unclassified - unlimited		
19. Security Classif. (of this report) Unclassified	20. Security Classif. (of this page) Unclassified		21. No. of Pages 20	22. Price* $3.00

Page Intentionally Left Blank

ROLE OF PLASTIC DEFORMATION IN WEAR OF COPPER AND COPPER-

10-PERCENT-ALUMINUM ALLOY IN CRYOGENIC FUELS

by Robert C. Bill and Donald W. Wisander

Lewis Research Center and
U.S. Army Air Mobility R&D Laboratory

SUMMARY

This investigation is a study of the wear mechanisms that operate in high-purity cop-
per specimens and a copper - 10-percent-aluminum alloy specimen subjected to sliding
against 440C in environments of liquid methane and liquid natural gas, respectively.
Also, one high-purity copper specimen was subjected to sliding in liquid hydrogen. The
specimens were in the form of a hemispherically tipped copper or copper alloy rider in
contact with a 440C disk.

Scanning electron microscopy examinations of the rider wear scar surfaces were
made after sliding at 12.4 meters per second under a 1-kilogram normal load. Wear
rate measurements were made during experiments at 3.1, 6.2, and 12.4 meters per
second under normal loads of 1/2 and 1 kilogram.

The results showed that nearly all the wear occurred by plastic deformation of a re-
crystallized layer extending to a depth of the order of 10 micrometers below the wear
scar surface on the rider. The wear debris was in the form of a layered structure ad-
hering to the exit side of the rider wear scar. Very little rider material transferred to
the 440C disk or became loose debris. Measurements under the various speed and load
conditions showed that the wear rate was proportional to the sliding velocity squared and
to the normal load. A physical model of the wear process is proposed to account for
these observations.

INTRODUCTION

Plastic flow in friction and wear is usually considered as forming a crucial step in
the development of adhesive junctions (refs. 1 to 3). The simplest concept of the impor-
tance of plastic flow is that yielding of the contacting asperities will continue until the

contact area has grown to such an extent that the local contact stress has decreased to the yield stress of the material. Basically, this explains the significance of the hardness term in Archard's wear equation (ref. 2), $\dot{w} = K(LV/H)$, where L is the load, H the hardness, V the sliding velocity, and K a material constant. In addition to the growth of the contact area under normal load, further junction growth occurs with the addition of the frictional force, leading to a significant increase in contact area and friction (refs. 1 and 3). The role of plasticity in friction and wear has been further discussed in the work of Antler (refs. 4 to 6) and Cocks (refs. 7 and 8). They showed that, following the adhesion and junction growth process, plastic flow occurred in the bulk of the metal, producing a wedge formation of cold-worked metal. As sliding continued, the cold-worked formation was seen either to form a loose wear particle or to readhere to one of the sliding surfaces. A good geometric description of the wedge flow mechanism is given in reference 8. Briefly, it proceeds when a junction, inclined in the direction of relative motion, forms between the two surfaces. The shear forces applied across the inclined junction result in the shear of the bulk metal ahead of the junction. The process is similar to machining on a very fine scale, with the exception that plastic deformation may occur in both contacting bodies.

The objectives of this report are to describe a plastic deformation process observed in the sliding wear of 99.95-percent copper and copper - 10-percent aluminum against 440C in cryogenic liquids (liquid methane, liquid natural gas, and liquid hydrogen), and to develop a model that accounts for the observed wear rates.

There are two important differences between the previously cited work of Antler and Cocks and the work that is described in this report. First, the experiments of Antler and Cocks involved sliding between soft metal pairs, typically aluminum on aluminum or gold on gold, rather than a soft metal (copper) sliding against a very hard metal (400C). The second difference involves environmental conditions and test parameters. Prior work was conducted in air at room temperature with very low sliding speeds (0.033 cm/sec in the case of Cocks, and 1 cm/sec in the case of Antler), whereas the work reported herein was performed in a cryogenic, nonoxidizing environment at sliding speeds from 3.1 to 12.4 meters per second.

The sliding-pair combinations and experimental environment of this investigation were selected on the basis of the materials being candidates for rolling-element bearing cages in cryogenic pump applications.

SYMBOLS

A   real area of contact

A'   apparent area of contact

D	average diameter of contacting asperities (or events)
H	hardness
h	mean thickness of recrystallized layer
h_o	reference thickness of recrystallized layer
K	material constant (wear coefficient)
k	yield shear stress
L	applied normal load
$\dot{N}$	number of events crossing exit line per unit time
V	sliding velocity
V_o	reference velocity
$\dot{W}$	wear rate of rider
μ	coefficient of friction
τ_{xy}	shear stress in sliding direction
σ_{xx}	normal stress on wear scar surface, in loading direction
σ_{zz}	normal stress on wear scar surface, transverse to loading and sliding directions
σ_1	algebraically smallest principal stress
σ_2	algebraically largest principal stress
σ_3	intermediate principal stress

APPARATUS AND PROCEDURE

The apparatus used in this study is shown in figure 1 and is more completely described in reference 9. The basic elements consisted of a hemispherically tipped 4.76-millimeter-radius rider specimen held in sliding contact with the lower flat surface of a 63.5-millimeter-diameter rotating disk. The experiments were conducted with specimens completely submerged in liquified cryogenic fuel. The sliding speed was 12.4 meters per second (4100 rpm). The rider specimen was loaded to 1 kilogram against the rotating disk by a helium-pressurized bellows assembly. The frictional force and the normal load were measured by strain-gage dynamometer rings.

The test chamber was cleaned with 90 percent ethanol before each run. After cleaning and the installation of the specimens, the test chamber was closed, purged for 15 minutes with helium gas, and then filled with liquified cryogenic fuel. After the test

chamber was full and the liquid boiling had stabilized, the rider specimen was loaded against the rotating disk. The duration of the runs was 1/2 hour.

The disk specimen preparation was as follows: The surfaces were (1) finish ground and lapped to 5×10^{-2} micrometer rms (2 μin. rms), (2) scrubbed with moist levigated alumina, (3) washed in tap water, (4) washed in distilled water and air dried.

The copper specimens were of 99.95 percent purity, and the copper and aluminum used to cast the copper - 10-percent-aluminum alloy were each of 99.999 percent purity.

RESULTS AND DISCUSSION

Microscopic Description of Wear Scars

The general features of the layered buildup of wear material on copper - 10-percent-aluminum run in liquid natural gas are shown in figure 2. The formation is divided into three major buildups growing radially outward from the edge of the contact area. The outline of the circular contact area on the exit side of the scar is faintly discernible through the topmost layer. The variations in shading (dark and light patches) within the contact area are caused by minor undulations of the surface.

The material in the layered formations was collected, weighed, and compared with the theoretical weight of the material that was originally in the wear scar volume. These weights were found to be very nearly equal, indicating that the bulk of the material originally in the wear scar volume was transferred to the layered formations by some mechanism. Very little of the copper - 10-percent aluminum could have been transferred to the 440C disk or lost as wear debris. Also, in the nonoxidizing cryogenic environment, little chemical wear could have occurred; and surface ductility may have been enhanced.

In the case of the experiment with high-purity copper, the layer formation was generally similar to that just described. The bulk of the material originally comprising the wear volume was again found to be in the layered formation after sliding.

The details shown in the scanning electron microscope (SEM) photographs of figures 3 and 4 reveal that the layer structure results from the shearing of large areas over the exit line of the wear scar. In figures 3(a) and (c) and 4(a), the topmost layers may be seen having just crossed the exit line. The high-magnification exposure of figure 3(b) shows that each layer is about 30 micrometers long (in the direction of sliding) and a few micrometers thick. The dimensions and regularity of the layers are not likely to have been the result of a wedge-flow wear mechanism. Considering the hardness of the 440C disk (56 Rockwell C), plowing by the asperities on the disk would be expected rather than the wedge flow mechanism. Indeed, some fine scratches indicative of plowing may be seen on the rider wear scars, but there is little relationship between the scratches and the size and distribution of the layers. These considerations, combined with the obser-

4

vation that there was little material transfer or loose debris generation, lead to the conclusion that the wear mechanism involves the plastic flow of fairly large areas of the surface of the wear scar.

The high-purity copper specimen was sectioned, polished, and etched to reveal the grain structure beneath the wear scar surface; the section photographs are shown in figure 5. The material beneath the wear scar is composed of two distinct layers. The uppermost layer is composed of fine-grained (about 5-μm grain diameter) recrystallized copper extending to a depth of 10 to 15 micrometers near the exit and diminishing to zero depth near the entrance region. Directly beneath this recrystallized layer is a region of severely cold-worked metal, extending to a 50-micrometer depth at the exit region and vanishing near the entrance.

Usually, the recrystallization temperature of copper is considered to be 300° to 400° C, but this temperature is greatly affected by the degree of prior cold work and the temperature at which the cold work occurred. Hence, one cannot be certain about the temperature reached in the recrystallized surface layer. Judging from the grain size though, the layer is probably continuously being worked and recrystallized, allowing no time for secondary recrystallization and grain growth to occur. In any case, the effect that the recrystallized layer has on the surface mechanical properties is one of lowering the yield stress to the level of annealed copper (about 2 kg/mm^2 shear) and thus limiting the amount of strain hardening that may occur and generally promoting ductility. Thus, the plastic flow that occurs in the wear-scar surface region must take place mostly in the recrystallized layer. An important effect that the cryogenic environment may have had was to limit the depth to which recrystallization occurred.

Description of Wear Mechanism

Figure 6 illustrates the stress state of a material element near the wear surface of the rider. The element is compressed in the y-direction by the normal applied load, and it is subjected to x-y shear by the frictional force associated with the normal load. The element is assumed to be constrained in the lateral (z) direction by surrounding material. These conditions essentially describe a plane-strain situation with the principal axes inclined to the designated x-y direction. In figure 2, the plane-strain supposition appears to be reasonable since most visible material movement is directly toward the exit, except for some lateral movement at either side of the exit region.

In the sliding friction case considered here,

$$\sigma_{xx} = \frac{L}{A}$$

where

L   applied normal load

A   real area of contact

From plane-strain considerations (ref. 10),

$$\sigma_{zz} = -\frac{1}{2}\sqrt{\sigma_{xx}^2 + 4\tau_{xy}^2}$$

where

$$\tau_{xy} = \mu\sigma_{xx}$$

and μ is the coefficient of friction.

The principal stresses may now be found, permitting the conditions under which yielding may occur to be identified:

$$\left.\begin{aligned}
\sigma_1 &= -\left(\frac{1}{2}\sigma_{xx} + \frac{1}{2}\sqrt{\sigma_{xx}^2 + 4\tau_{xy}^2}\right) \\[2mm]
\sigma_2 &= -\left(\frac{1}{2}\sigma_{xx} - \frac{1}{2}\sqrt{\sigma_{xx}^2 + 4\tau_{xy}^2}\right) \\[2mm]
\sigma_3 &= -\frac{1}{2}\sqrt{\sigma_{xx}^2 + 4\tau_{xy}^2}
\end{aligned}\right\} \tag{1}$$

According to the Tresca yield criterion, yield occurs when the maximum shear stress equals the yield shear stress or, in terms of principal stresses, when

$$\sigma_1 - \sigma_2 = 2k \tag{2}$$

where k is the yield shear stress.

One can now arrive at an estimate of the wear-scar surface area undergoing shear at a given time. Combining equations (1) and (2) gives $2k = \sigma_{xx}\sqrt{1 + 4\mu^2}$, giving

$$A = \frac{L}{2k}\sqrt{1 + 4\mu^2} \tag{3}$$

Using a value of 2 kilograms per millimeter squared for k and the observed value of 0.6 to 0.7 for μ gives the actual area of contact as being about 0.4 square millimeter under

6

a 1-kilogram normal load, or about 5 percent of the wear scar area as measured after an experiment. Thus, a nonuniform mechanism operating over only a small fraction of the surface at a time resulted in the transport of material across the wear scar surface. The nonuniform wear mechanism may be described by the following process.

On any surface subjected to sliding contact, surface asperities are always present and can in fact continuously arise from thermal effects. The deformation of an asperity under combined loading may again be approximately treated by plane-strain techniques (ref. 11). Figure 7 shows a slip line field adapted from the plane-strain indentation problem after Hill (ref. 9), taking into account a surface shearing force that is characteristic of a sliding interface. The associated velocity vector diagram indicates that material is forced out from under the contact zone, preferentially in the sliding direction. As deformation proceeds, the contact area grows, which reduces the stress level and decreases the rate of deformation. Thermal contraction then leads to a localized surface recession. The sequence of deformation, contact area growth, and thermal recession is depicted in figure 8. In this way, material is transported toward the exit line of the wear scar by plastic deformation, with the accompanying recession of the wear scar surface. A given element of material on the wear scar surface is subjected to such successive deformation mechanisms until it is sheared across the exit line of the wear scar, forming one of the flat layers seen in the adhering layer structures. This process of shear across the exit line is shown dramatically in the series of photographs of figure 9. As the layer buildup grows, wear-scar surface recession causes the junction between the first sheets formed and the edge of the wear scar to fail in shear, thus allowing the buildup to grow outward.

Parametric Model Describing Wear Rate

With the identification of a plausible wear mechanism, the first step was taken in developing a model for wear under the experimental sliding conditions. Wear measurements were made on five copper riders sliding against 440C in liquid methane under loads of 1/2 and 1 kilogram and at sliding speeds of 12.4, 6.2, and 3.1 meters per second. Wear rates were calculated after an equivalent sliding distance in each experiment and are shown in table I. The results of the calculations show that the wear rate is approximately proportional to the applied load and to the sliding velocity squared.

A model describing the measured wear rates can be developed by considering the number and extent of plastic shearing of deformation events crossing the exit line per unit time. The number of events crossing the exit line per unit time is proportional to the ratio of the sliding velocity V (which determines the average speed at which a surface element moves) to the spacing between events d. The value of d is given by

$$d \propto \frac{A'}{A/D} \tag{4}$$

where A' is the apparent contact area; A is the real contact area (given by eq. (3)); and D is the average diameter of contacting asperities, or events. Then the number of events crossing the exit line per unit time is given by

$$\dot{N} \propto \frac{VA}{A'D} = \frac{VL\sqrt{1 + 4\mu^2}}{2kDA'} \tag{5}$$

The extent of plastic deformation occurring per event is hard to quantify. It depends on the geometry of the contact and its slip line field, and it occurs largely in the recrystallized layer. If the depth of penetration of the slip line field on the exit half of the contact (see fig. 7) is initially smaller than the depth of the recrystallized layer, the contact area will grow in the sliding direction until the exit half of the slip line field penetrates to the cold-worked layer. Note that the deformation on the entrance half of the contact area is shut down sooner in the deformation process, since the entrance half of the slip line field initially penetrates to a greater depth, as shown in figure 7. For purposes of approximation then, the extent of deformation is assumed to be proportional to the recrystallized layer thickness h. In turn, the degree of recrystallization is determined by the rate of heat generation at the surface, which is proportional to V, the sliding velocity. Therefore, the term describing the extent of deformation occurring in a given event may be expressed as

$$\gamma \propto h = h_0 \frac{V}{V_0} \tag{6}$$

where h is the mean thickness of the recrystallized layer, and h_0 is the thickness of the recrystallized layer measured after sliding at velocity V_0.

The wear rate may now be expressed as the product of equations (5) and (6),

$$\dot{W} \propto \frac{V^2 L\sqrt{1 + 4\mu^2}\, h_0}{2kV_0 DA'} \tag{7}$$

Equation (7) does express the proportionality of wear rate to applied load and velocity squared. However, considerable development is needed to get it into a potentially useful form. As it now stands, there are two serious deficiencies. The terms h_0 and V_0 should not appear but should be expressed in terms of material properties in a way as yet

unknown. Also, the term D should be developed analytically. Further experimental work would also help to verify the model and to define the envelope of experimental conditions over which the LV^2 proportionality exists.

CONCLUDING REMARKS

Based on the combination of microscopic observation and wear measurements, the following statements may be made concerning the wear of copper and copper - 10-percent aluminum at cryogenic temperatures:

1. Virtually all the metal displaced by the sliding process was transported by plastic deformation to the exit of the wear scar, where it formed an adhering layer structure.

2. The bulk of the plastic shearing occurred in a recrystallized layer on the surface of the wear scar.

3. Wear rate measurements on copper specimens subjected to sliding in liquid methane indicate that over the loading range of 1/2 to 1 kilogram and over the range of sliding speeds of 12.4 to 3.1 meters per second, the wear rate is roughly proportional to load and velocity squared.

4. A mechanism was proposed describing the wear process as a series of intermittent plastic shearing events, eventually resulting in the transport of material across the exit line of the wear scar. Based on this mechanism, a model was partially developed which was in agreement with the wear measurements.

Lewis Research Center,
    National Aeronautics and Space Administration,
        and
U.S. Army Air Mobility R&D Laboratory,
        Cleveland, Ohio, February 1, 1973,
            501-24.

REFERENCES

1. Bowden, F. P.; and Tabor, D.: The Friction and Lubrication of Solids. Vol. 2. Clarendon Press, 1964, p. 74.

2. Archard, J. F.: Wear. Interdisciplinary Approach to Friction and Wear. NASA SP-181, 1968, pp. 267-333.

3. Buckley, Donald H.: The Influence of the Atomic Nature of Crystalline Materials on Friction. ASLE Trans., vol. 11, no. 2, Apr. 1968, pp. 89-100.

4. Antler, Morton: The Lubrication of Gold. Wear, vol. 6, 1963, pp. 44-65.

5. Antler, Morton: Processes of Metal Transfer and Wear. Wear, vol. 7, 1964, pp. 181-203.

6. Antler, Morton: Wear, Friction, and Electrical Noise Phenomena in Severe Sliding Systems. ASLE Trans., vol. 5, no. 2, Nov. 1962, pp. 297-307.

7. Cocks, M.: Shearing of Junctions Between Metal Surfaces. Wear, vol. 9, 1966, pp. 320-328.

8. Cocks, M.: Role of Displaced Metal in the Sliding of Flat Metal Surfaces. J. Appl. Phys., vol. 35, no. 6, June 1964, pp. 1807-1814.

9. Wisander, Donald W.: Friction and Wear of Selected Metals and of Carbons in Liquid Natural Gas. NASA TN D-6613, 1971.

10. Rowe, Geoffrey W.: An Introduction to the Principles of Metalworking. St. Martin's Press, 1965, p. 46.

11. Green, A. P.: The Plastic Yielding of Metal Junctions Due to Combined Shear and Pressure. J. Mech. Phys. Solids, vol. 2, no. 3, 1954, pp. 197-211.

TABLE I. - WEAR RATE OF 99.95 PERCENT

COPPER SUBJECTED TO 11×10^3 METERS

OF SLIDING CONTACT AGAINST 440C

IN LIQUID METHANE UNDER THE

SPECIFIED CONDITIONS

Load, kg	Sliding velocity, m/sec	Wear rate, cm^3/min
1/2	12.4	8.0×10^{-6}
1/2	6.2	1.5
1	12.4	14.0
1	6.2	3.5
1	3.1	[a]1.1

[a]After 5×10^3 meters.
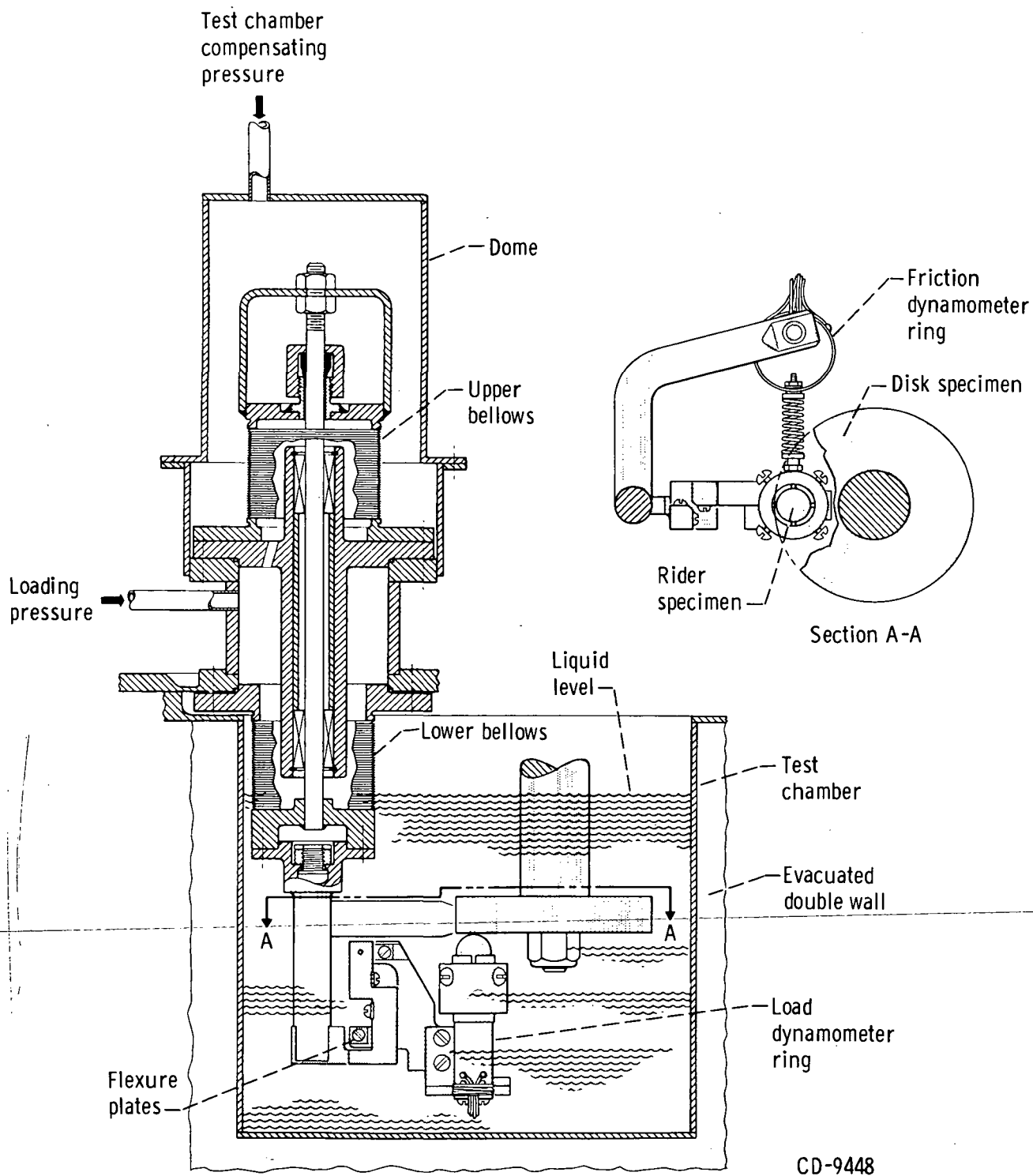
Figure 1. – Cryogenic fuel friction apparatus with specimen loading system.
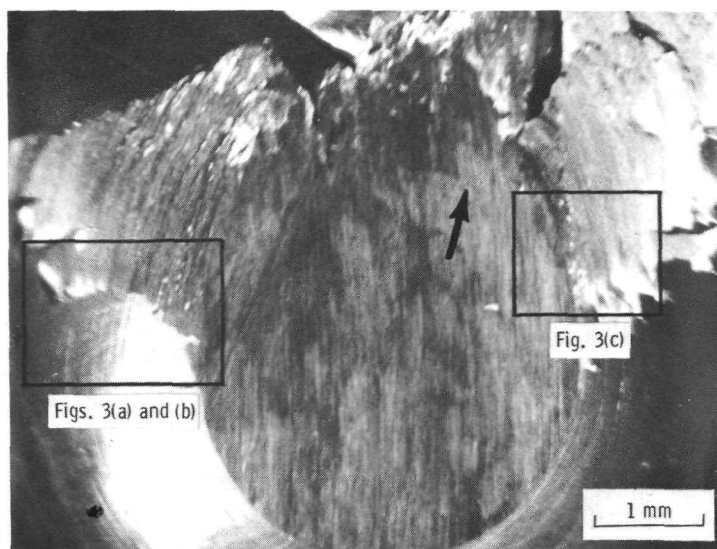
Entrance edge

Figure 2. - Wear scar produced on copper - 10-percent aluminum after sliding for 1/2 hour against 440C in liquid natural gas. Load, 1 kilogram; sliding velocity, 12.4 meters per second. Arrow points to circular outline of contact area, showing faintly through the adhering layered buildup.
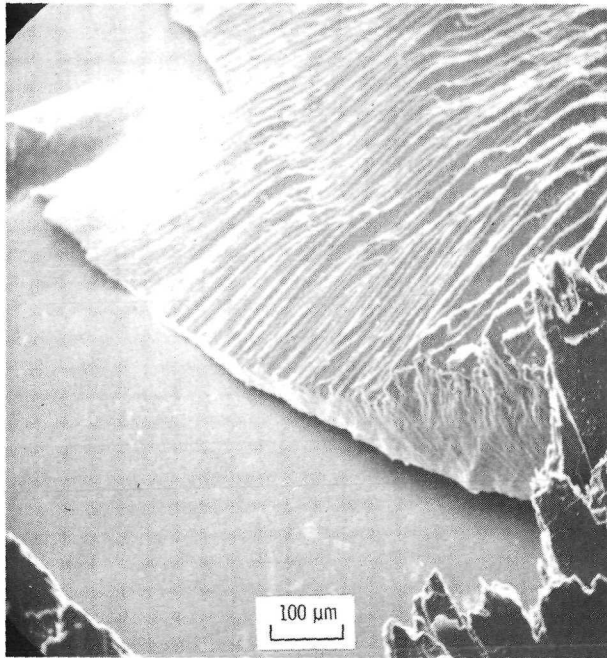
(a) Overview of layer stack.
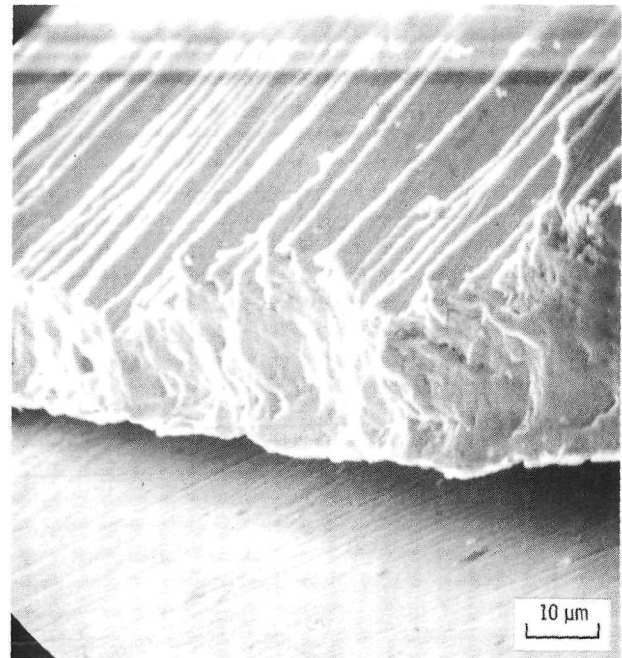
(b) Partial edge-on view of layer stack.
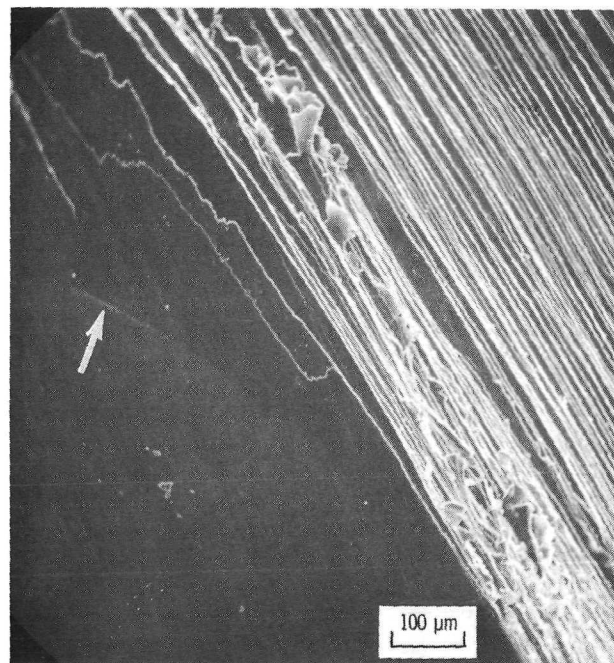
(c) Plan view of layer stack, showing edge of wear scar (indicated by arrow).

Figure 3. - Scanning electron micrograph photographs of layered buildup on copper - 10-percent aluminum after sliding against 440C in liquid natural gas at 12.4 meters per second under a 1-kilogram load.
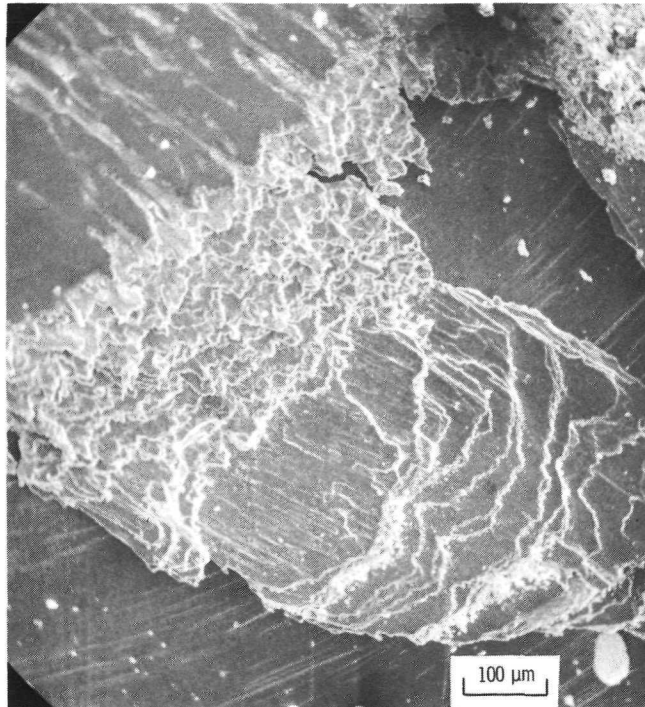
(a)
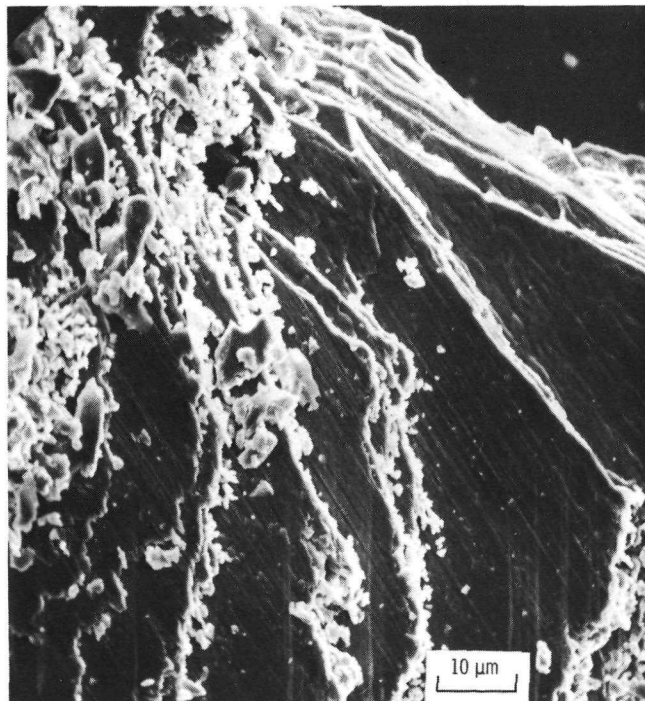
(b)

Figure 4. - Scanning electron micrograph photographs of layered buildup on high-purity copper after sliding against 440C in liquid hydrogen at 12.4 meters per second under a 1-kilogram load.
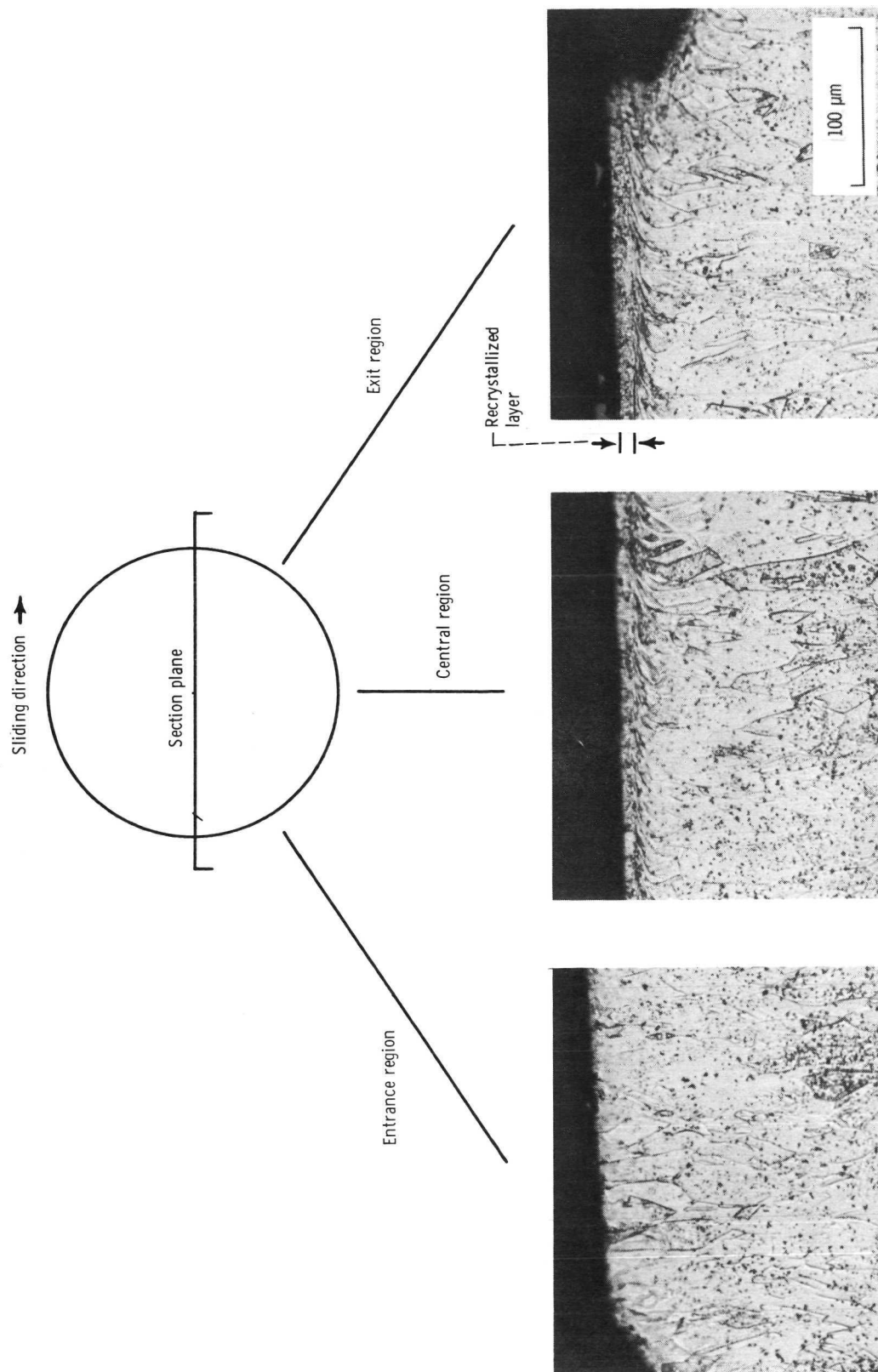
Figure 5. - Section micrographs of high-purity copper after sliding on 440C in liquid hydrogen at 12.4 meters per second under a 1-kilogram load.
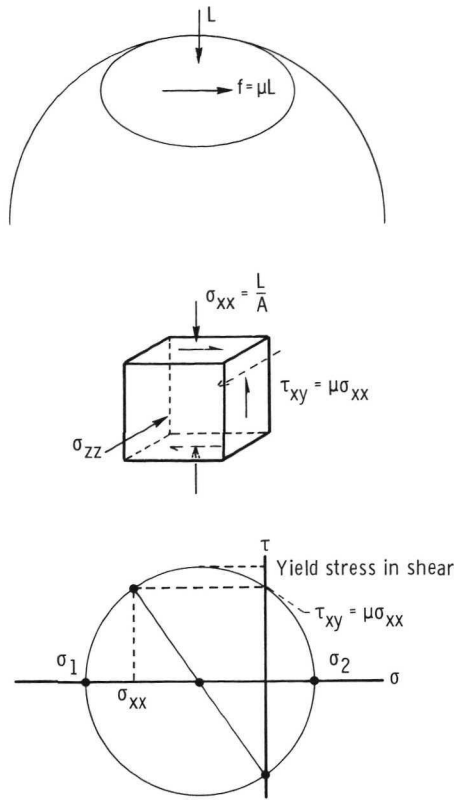
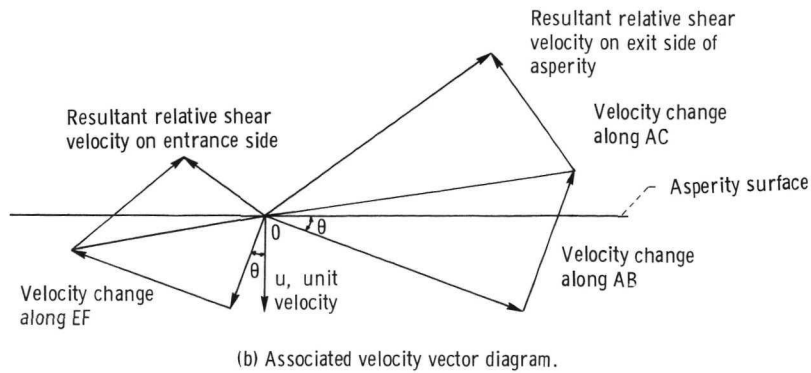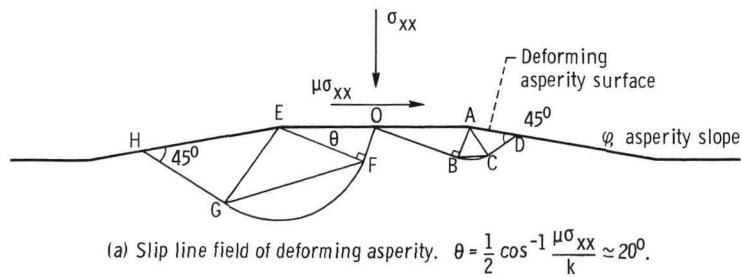Figure 6. – Stress state of surface element, illustrating conditions required for yield.
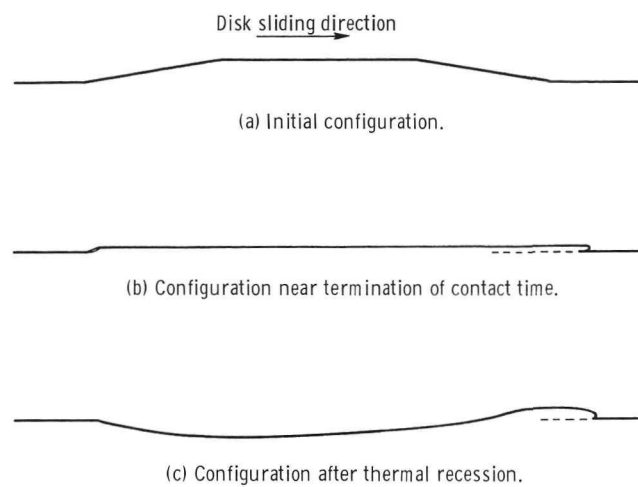

(a) Slip line field of deforming asperity. $\theta = \frac{1}{2} cos^{-1} \frac{\mu\sigma_{xx}}{k} \simeq 20^{0}$.

(b) Associated velocity vector diagram.

Figure 7. – Approximate slip line field solution of deforming asperity.

Disk sliding direction

(a) Initial configuration.

(b) Configuration near termination of contact time.

(c) Configuration after thermal recession.

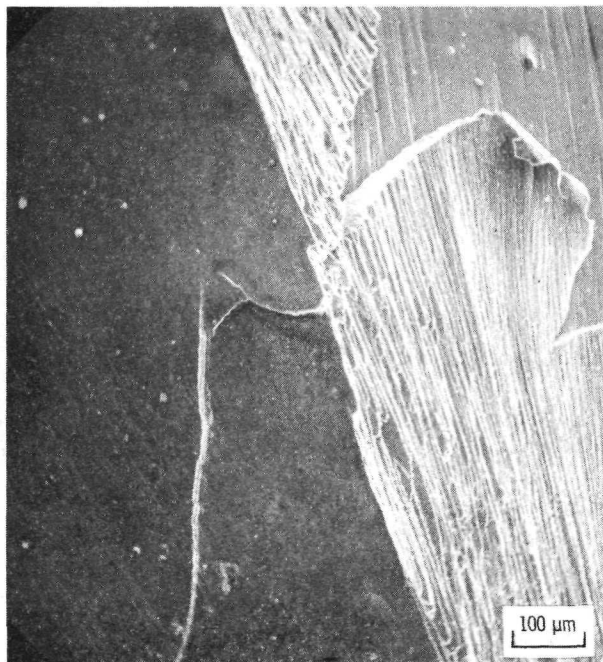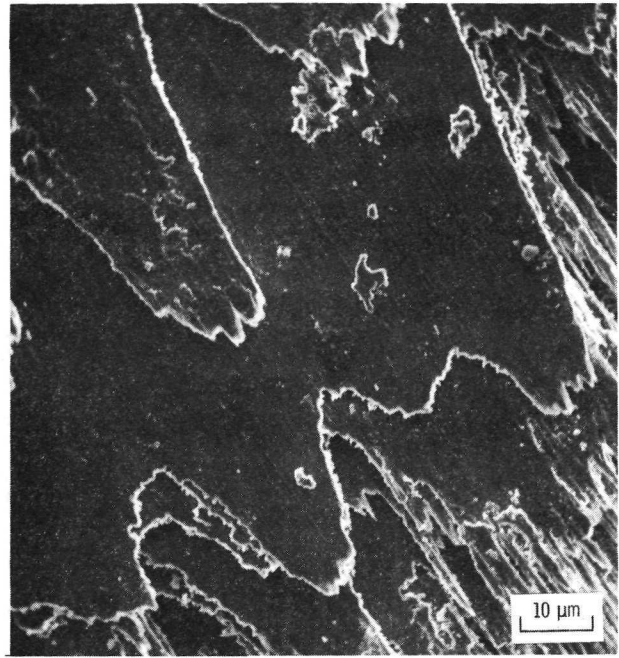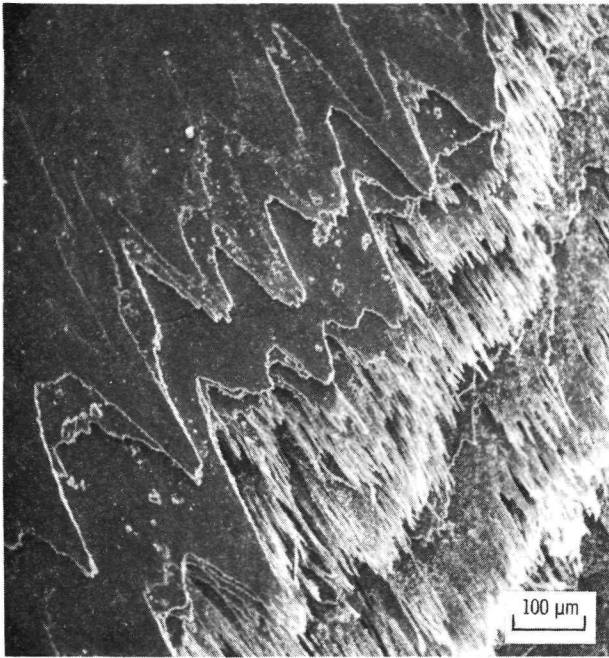Figure 8. - Sequence of deformation of contacting asperity.

Figure 9. – Scanning electron micrograph photographs of high-purity copper after sliding on 440C in liquid hydrogen at 12.4 meters per second under a 1-kilogram load.

Page Intentionally Left Blank

Page Intentionally Left Blank

"The aeronautical and space activities of the United States shall be conducted so as to contribute . . . to the expansion of human knowledge of phenomena in the atmosphere and space. The Administration shall provide for the widest practicable and appropriate dissemination of information concerning its activities and the results thereof."
—NATIONAL AERONAUTICS AND SPACE ACT OF 1958

NASA SCIENTIFIC AND TECHNICAL PUBLICATIONS

TECHNICAL REPORTS: Scientific and technical information considered important, complete, and a lasting contribution to existing knowledge.

TECHNICAL NOTES: Information less broad in scope but nevertheless of importance as a contribution to existing knowledge.

TECHNICAL MEMORANDUMS: Information receiving limited distribution because of preliminary data, security classification, or other reasons. Also includes conference proceedings with either limited or unlimited distribution.

CONTRACTOR REPORTS: Scientific and technical information generated under a NASA contract or grant and considered an important contribution to existing knowledge.

TECHNICAL TRANSLATIONS: Information published in a foreign language considered to merit NASA distribution in English.

SPECIAL PUBLICATIONS: Information derived from or of value to NASA activities. Publications include final reports of major projects, monographs, data compilations, handbooks, sourcebooks, and special bibliographies.

TECHNOLOGY UTILIZATION PUBLICATIONS: Information on technology used by NASA that may be of particular interest in commercial and other non-aerospace applications. Publications include Tech Briefs, Technology Utilization Reports and Technology Surveys.

Details on the availability of these publications may be obtained from:

SCIENTIFIC AND TECHNICAL INFORMATION OFFICE

NATIONAL AERONAUTICS AND SPACE ADMINISTRATION
Washington, D.C. 20546